International Journal of Bifurcation and Chaos, Vol. 29, No. 9 (2019) 1950117 (14 pages)

DOI: 10.1142/S0218127419501177

Multiscroll Hyperchaotic System with Hidden Attractors and Its Circuit Implementation

Xin Zhang* and Chunhua Wang†
College of Computer Science and Electronic Engineering, Hunan University, Changsha 410082, P. R. China
**zhangxin2302@126.com*
†*wch1227164@hnu.edu.cn*

Received July 12, 2018; Revised November 6, 2018

Based on the study on Jerk chaotic system, a multiscroll hyperchaotic system with hidden attractors is proposed in this paper, which has infinite number of equilibriums. The chaotic system can generate $N+M+2$ scroll hyperchaotic hidden attractors. The dynamic characteristics of the multiscroll hyperchaotic system with hidden attractors are analyzed by means of dynamic analysis methods such as Lyapunov exponents and bifurcation diagram. In addition, we have studied the synchronization of the system by applying an adaptive control method. The hardware experiment of the proposed multiscroll hyperchaotic system with hidden attractors is carried out using discrete components. The hardware experimental results are consistent with the numerical simulation results of MATLAB and the theoretical analysis results.

Keywords: Multiscroll; hyperchaotic; hidden attractor; adaptive synchronization; hardware experiment.

1. Introduction

In the past, chaos has been widely studied for its complex and interesting nonlinear dynamic behaviors [Lorenz, 1963; Chua *et al.*, 1986; Sprott, 2000]. Chaos has been proved to be applicable to various fields, such as neural networks [Swathy & Thamilmaran, 2014], image encryption [Boriga *et al.*, 2014; Wang & Zhang, 2016; Zhou *et al.*, 2018a] and secure communication [Filali *et al.*, 2014; Wu *et al.*, 2015].

In order to increase the dynamic complexity of chaotic system and better apply it to related fields, the related researchers have constructed a variety of complex chaotic systems [Pham *et al.*, 2015; Zhang *et al.*, 2018; Bao *et al.*, 2018]. The multiscroll and multiwing hyperchaotic systems have been studied extensively because of their complex dynamic characteristics [Wang *et al.*, 2017a; Wang *et al.*, 2017c; Bao *et al.*, 2017; Zhang & Wang, 2019; Zhou *et al.*, 2016, 2017].

From the perspective of calculation, attractors in chaotic systems can be divided into two types: self-excited attractors and hidden attractors [Leonov & Kuznetsov, 2013]. The chaotic system with hidden attractors was first found and analyzed in [Leonov *et al.*, 2011]. The general definition of chaotic system with hidden attractors is that the hidden attractor has a basin of attraction that does not intersect with neighborhoods of equilibriums [Leonov *et al.*, 2011, 2012; Leonov & Kuznetsov, 2013; Leonov *et al.*, 2014]. According to the number and type of equilibriums, the chaotic system with hidden attractors includes three main types: hidden attractor with only stable equilibrium, hidden attractor without equilibrium, and hidden attractor with infinite number of equilibriums [Pham *et al.*, 2017a]. The chaotic systems with only stable equilibrium were proposed in [Molaie *et al.*, 2013; Wang & Chen, 2012] and [Wang *et al.*, 2017b],

†Author for correspondence

where 23 chaotic systems with only stable equilibrium were found in [Molaie *et al.*, 2013], aided by computer search algorithms. Similarly, using computer search algorithms, 17 chaotic systems without equilibrium were discovered [Jafari *et al.*, 2013]. Some other diverse chaotic or hyperchaotic systems without equilibrium were reported in [Borah & Roy, 2017; Pham *et al.*, 2017b; Wang & Chen, 2012; Wang *et al.*, 2012; Khan & Shikha, 2018; Singh & Roy, 2018; Hu *et al.*, 2016; Hu *et al.*, 2017; Escalante-Gonzalez *et al.*, 2017]. According to the published literatures, the chaotic or hyperchaotic systems with infinite number of equilibriums include the following types (including but not limited to): the equilibriums linearly distributed [Zhou *et al.*, 2013; Jafari & Sprott, 2013; Zhou & Yang, 2013]; circularly distributed [Gotthans & Petrzela, 2015]; squarely distributed [Gotthans *et al.*, 2016]; elliptically distributed [Pham *et al.*, 2016a] and curvilinear distributed [Chen & Yang, 2015; Pham *et al.*, 2016b].

On the whole, in the literatures that have been reported, the chaotic systems with hidden attractors that can generate any number of scrolls are not hyperchaotic, whereas the hyperchaotic systems with hidden attractors cannot generate any number of scrolls. So far, no literature has reported a multiscroll hyperchaotic system with hidden attractors, and the reported multiscroll chaotic systems with hidden attractors have the disadvantage of being unfavorable to circuit implementation.

Compared with general chaotic systems with hidden attractors, multiscroll hyperchaotic systems with hidden attractors have more complex dynamic characteristics, so they are more suitable for the application of chaotic secure communication and chaotic image encryption, etc. However, it is hard to obtain multiscroll hyperchaotic systems with hidden attractors by using the general method of constructing multiscroll chaotic systems. Therefore, researching how to construct multiscroll hyperchaotic systems with hidden attractors can not only enrich the types of chaotic systems used in chaotic secure communication, chaotic image encryption and other applications, but can also further promote the researchers' understanding of chaotic systems with hidden attractors. It is still necessary to study how to use the existing chaotic systems to obtain multiscroll hyperchaotic systems with hidden attractors that are easy to be implemented by circuits. Therefore, it is of great significance to study multiscroll hyperchaotic systems with hidden attractors and this paper is carrying out the related research.

The next section describes the mathematical model of the new multiscroll hyperchaotic system with hidden attractors. The dynamic characteristics and the synchronization example of the system are studied in Sec. 3. We conduct the hardware circuit design and show the experimental results in Sec. 4. Section 5 reports the comparison of relevant literatures. Finally, the conclusion of the overall study is given in the last section.

2. Multiscroll Hyperchaotic System with Hidden Attractors

On the basis of Jerk system [Sprott, 2000], we propose a multiscroll hyperchaotic system with hidden attractors and its state equation is

$$\begin{cases} \dfrac{dx}{d\tau} = y, \\ \dfrac{dy}{d\tau} = z - \alpha yzw, \\ \dfrac{dz}{d\tau} = -x - y - \beta z + f(x, M, N), \\ \dfrac{dw}{d\tau} = y + z, \end{cases} \tag{1}$$

where α, β are two constant coefficients of the system state equation, $f(x, M, N)$ is a step sequence with the middle point of its vertical edge located at the origin of the coordinate axis, and

$$\begin{aligned} f(x, M, N) &= 0.5\,\mathrm{sgn}(x) + 0.5\sum_{n=1}^{N}[\mathrm{sgn}(x-n)+1] \\ &\quad + 0.5\sum_{m=1}^{M}[\mathrm{sgn}(x+m)-1] \\ &= 0.5\left(N - M + \mathrm{sgn}(x) + \sum_{n=1}^{N}\mathrm{sgn}(x-n) \right. \\ &\quad \left. + \sum_{m=1}^{M}\mathrm{sgn}(x+m)\right). \end{aligned} \tag{2}$$

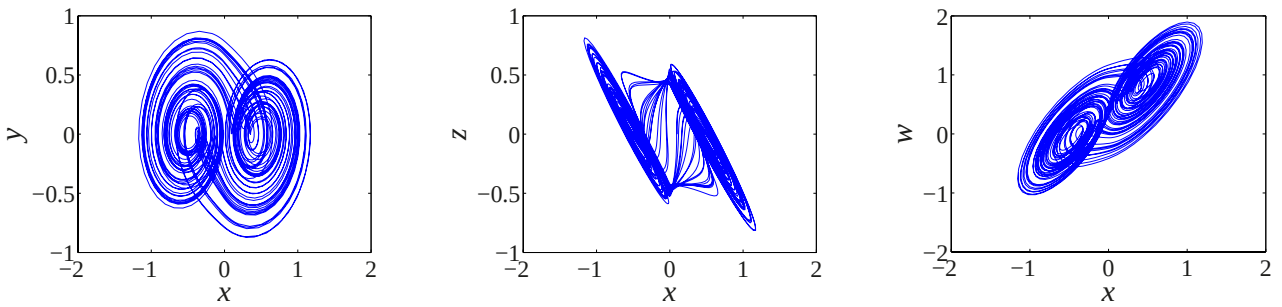

(a) (b) (c)

Fig. 1. Phase portraits of 2-scroll hyperchaotic hidden attractors in (a) x–y, (b) x–z and (c) x–w plane. The parameters are set as: $\alpha = 0.01$, $\beta = 0.62$, $N = M = 0$.

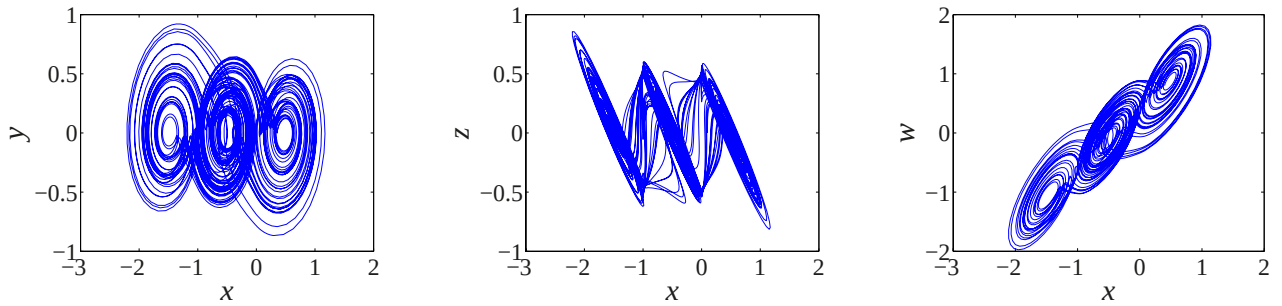

(a) (b) (c)

Fig. 2. Phase portraits of 3-scroll hyperchaotic hidden attractors in (a) x–y, (b) x–z and (c) x–w plane. The parameters are set as: $\alpha = 0.01$, $\beta = 0.62$, $N = 0$, $M = 1$.

If the appropriate values of α and β are selected, system (1) will generate $N + M + 2$ scroll hyperchaotic hidden attractors. Let $\alpha = 0.01$, $\beta = 0.62$, $N = M = 0$, system (1) will generate 2-scroll hyperchaotic hidden attractors, as shown in Fig. 1. When $N = 0$, $M = 1$, the phase portraits of the generated 3-scroll hyperchaotic hidden attractors are shown in Fig. 2. When $N = M = 1$, system (1) will generate 4-scroll hyperchaotic hidden attractors, as shown in Fig. 3. When $N = 1$, $M = 2$ and $N = M = 2$, system (1) will generate 5- and 6-scroll hyperchaotic hidden attractors, and the phase portraits are respectively shown in Figs. 4 and 5. When $N = 5$, $M = 6$, system (1) will generate 13-scroll hyperchaotic hidden attractors, as shown in Fig. 6. As can be seen from these phase portraits, by adjusting the values of the parameters N and M, the system (1) can generate different numbers of multiscroll hyperchaotic attractors with hidden characteristics along with the x-axis.

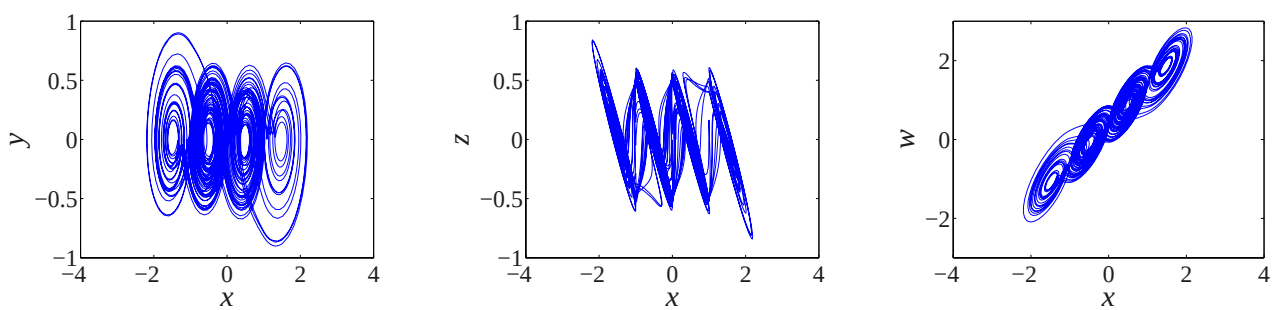

(a) (b) (c)

Fig. 3. Phase portraits of 4-scroll hyperchaotic hidden attractors in (a) x–y, (b) x–z and (c) x–w plane. The parameters are set as: $\alpha = 0.01$, $\beta = 0.62$, $N = M = 1$.

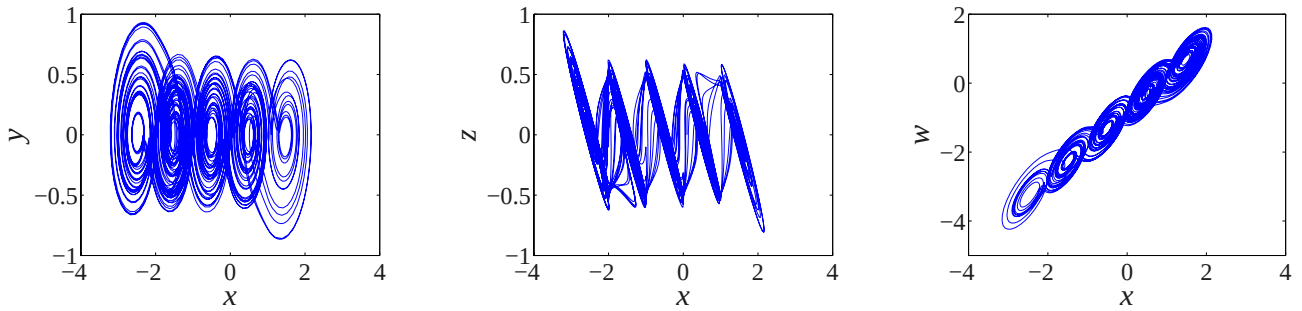

(a) (b) (c)

Fig. 4. Phase portraits of 5-scroll hyperchaotic hidden attractors in (a) x–y, (b) x–z and (c) x–w plane. The parameters are set as: $\alpha = 0.01$, $\beta = 0.62$, $N = 1$, $M = 2$.

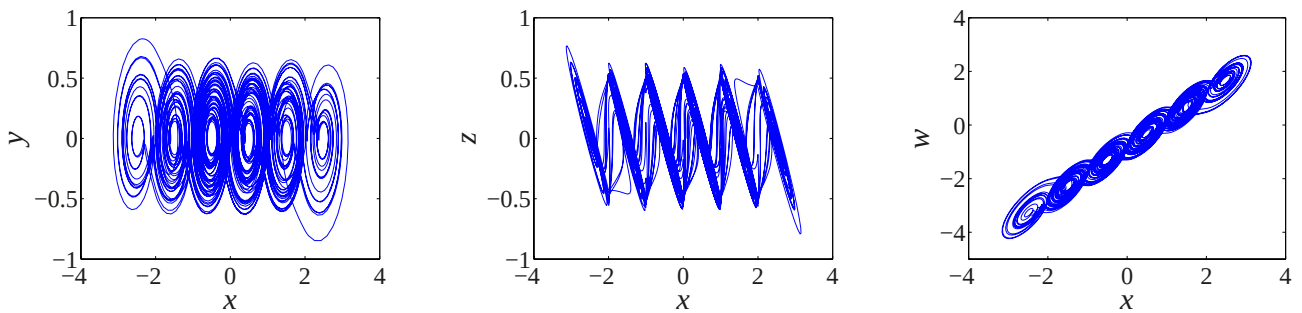

(a) (b) (c)

Fig. 5. Phase portraits of 6-scroll hyperchaotic hidden attractors in (a) x–y, (b) x–z and (c) x–w plane. The parameters are set as: $\alpha = 0.01$, $\beta = 0.62$, $N = M = 2$.

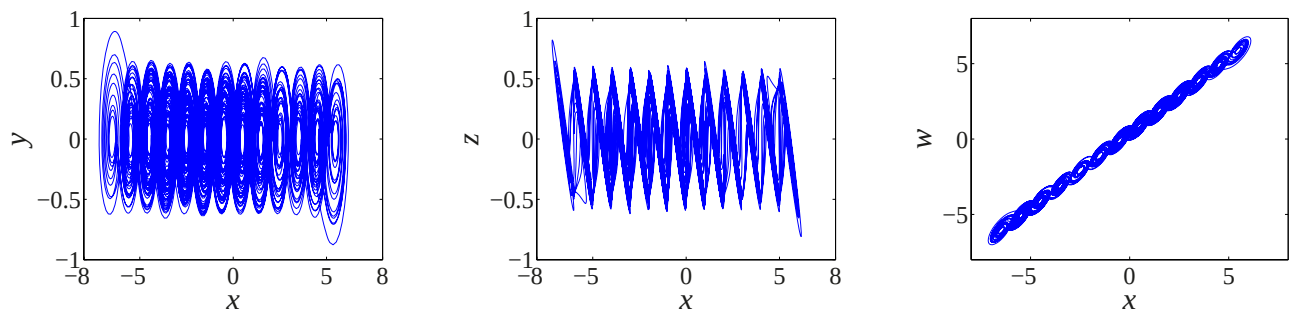

(a) (b) (c)

Fig. 6. Phase portraits of 13-scroll hyperchaotic hidden attractors in (a) x–y, (b) x–z and (c) x–w plane. The parameters are set as: $\alpha = 0.01$, $\beta = 0.62$, $N = 5$, $M = 6$.

3. Dynamics Analysis and Adaptive Synchronization

3.1. *Symmetry and dissipation*

System (1) has a natural symmetry under the coordinates transform (x, y, z, w) to $(-x, -y, -z, -w)$, which persists for all values of the system parameters. By using this property, it is easy to extend the saddle-focus equilibriums with index 2 by constructing multipiecewise functions with odd symmetric.

The general case of dissipativity for system (1) is calculated as

$$\nabla V = \frac{\partial \dot{x}}{\partial x} + \frac{\partial \dot{y}}{\partial y} + \frac{\partial \dot{z}}{\partial z} + \frac{\partial \dot{w}}{\partial w} = \alpha z w - \beta. \quad (3)$$

Therefore, system (1) is dissipative if $\nabla V < 0$, namely $\alpha zw - \beta < 0$, when selecting $\alpha = 0.01$, $\beta = 0.62$, and then we get $zw < 62$. This means that the asymptotic motion settles onto an attractor and each volume containing the system trajectory shrinks to zero at an exponential rate as $t \to \infty$.

3.2. *Equilibrium and stability analysis*

The equilibrium of system (1) can be obtained by solving the following equation

$$\begin{cases} y = 0, \\ z - \alpha yzw = 0, \\ -x - y - \beta z + f(x, M, N) = 0, \\ y + z = 0. \end{cases} \tag{4}$$

The equilibrium of system (1) is $E^Q = (x^E, y^E, z^E, w^E) = (x^E, 0, 0, c)$, where c is a real constant, $x^E = -M - 0.5, -M + 0.5, \ldots, -0.5, 0.5, \ldots, N - 0.5, N + 0.5$. It means that the w-axis is the line equilibrium of system (1), namely that system (1) has infinite number of equilibriums. According to the definition of chaotic system with hidden attractors [Jafari & Sprott, 2013; Pham *et al.*, 2016b], system (1) is a kind of chaotic system with hidden attractors. The Jacobian matrix of system (1) at the equilibrium E^Q can be expressed as

$$\begin{aligned} &J(E^Q) \\ &= \begin{bmatrix} 0 & 1 & 0 & 0 \\ 0 & \alpha zw & 1 - \alpha yw & \alpha yz \\ -1 + f'(x, M, N) & -1 & -\beta & 0 \\ 0 & 1 & 1 & 0 \end{bmatrix}\Bigg|_{E^Q} \\ &= \begin{bmatrix} 0 & 1 & 0 & 0 \\ 0 & 0 & 1 & 0 \\ -1 & -1 & -\beta & 0 \\ 0 & 1 & 1 & 0 \end{bmatrix}. \end{aligned} \tag{5}$$

It can be seen from Eq. (5) that, although the system (1) has infinite number of equilibriums, the Jacobian matrix at the equilibriums of this system is independent of the position of the equilibriums.

By solving $|\lambda \mathbf{E} - J(E^Q)| = 0$, where $\mathbf{E}$ is an identity matrix, we can get that the characteristic roots of the system (1) at the equilibrium E^Q satisfy the following equation

$$\lambda(\lambda^3 + \beta\lambda^2 + \lambda + 1) = 0. \tag{6}$$

Obviously, one of the solutions in Eq. (6) is 0, and the other three satisfy

$$\lambda^3 + \beta\lambda^2 + \lambda + 1 = 0. \tag{7}$$

The solution of Eq. (7) can be obtained according to the root formula of the standard unary cubic equation. The algebra expression of the general solution is

$$\begin{cases} \lambda_1 = -\dfrac{\beta}{3} + \sqrt[3]{-\dfrac{q}{2} + \sqrt{\Delta}} + \sqrt[3]{-\dfrac{q}{2} - \sqrt{\Delta}}, \\ \lambda_{2,3} = -\dfrac{\beta}{3} - \dfrac{1}{2}\left(\sqrt[3]{-\dfrac{q}{2} + \sqrt{\Delta}} + \sqrt[3]{-\dfrac{q}{2} - \sqrt{\Delta}}\right) \\ \qquad\quad \pm \dfrac{\sqrt{3}}{2} j \left(\sqrt[3]{-\dfrac{q}{2} + \sqrt{\Delta}} - \sqrt[3]{-\dfrac{q}{2} - \sqrt{\Delta}}\right), \end{cases} \tag{8}$$

where $q = 2\beta^3/27 - \beta/3 + 1, \Delta = q^2/4 + p^3/27 = \beta^3/27 - \beta^2/108 - \beta/6 + 31/108, p = -\beta^2/3 + 1$. According to the root criterion of the unary cubic equation, when $\Delta > 0$, the equation has a real root and two complex roots. Therefore, for ensuring that the system (1) has chaotic behavior, it must guarantee $\Delta > 0$. In addition, since the saddle-focus equilibrium with index 2 is extremely important for the generation of chaos, it is necessary to ensure that the solution of Eq. (7) has a negative real number solution and a pair of conjugate solutions with positive real parts, namely

$$\begin{cases} \Delta > 0, \\ -\dfrac{\beta}{3} + \sqrt[3]{-\dfrac{q}{2} + \sqrt{\Delta}} + \sqrt[3]{-\dfrac{q}{2} - \sqrt{\Delta}} < 0, \\ -\dfrac{\beta}{3} - \dfrac{1}{2}\left(\sqrt[3]{-\dfrac{q}{2} + \sqrt{\Delta}} + \sqrt[3]{-\dfrac{q}{2} - \sqrt{\Delta}}\right) > 0. \end{cases} \tag{9}$$

We can solve this equation and obtain $-2.6107186 < \beta < 1$, namely when system coefficient β meets this condition, Eq. (7) has a negative real number solution and a pair of conjugate solutions with positive real parts. We select $\beta = 0.62$, the solutions of Eq. (6) are $\lambda_1 = -0.8423, \lambda_{2,3} = 0.1111 \pm 1.0839j, \lambda_4 = 0$. In this case, all the equilibriums of the system are saddle-focus equilibriums

with index 2. Therefore, the system has the potential to generate a chaotic attractor.

3.3. *Lyapunov exponent, bifurcation diagram and Poincaré map*

In this section, we will use the dynamic analysis methods, including Lyapunov exponent diagram, bifurcation diagram and Poincaré map, to investigate the dynamical characteristics of the multiscroll hyperchaotic system with hidden attractors. Since the nonlinear function $f(x, M, N)$ in the proposed hyperchaotic system contains sign functions $\mathrm{sgn}(x)$, $\mathrm{sgn}(x-n)$ and $\mathrm{sgn}(x+m)$, in order to calculate the Lyapunov exponents, the continuous differentiable functions $a\tan(B(x))/(\pi/2), a\tan(B(x-n))/(\pi/2)$ and $2a\tan(B(x+m))/(\pi/2)$ are adopted to approximate the corresponding sign function. In general, if B is larger, the approximation performance is better, so $B = 1000$ is selected [Zhang & Yu, 2013; Zhou *et al.*, 2018b]. We use the famous Wolf algorithm [Wolf *et al.*, 1985] to simulate the Lyapunov exponent spectrum with respect to β. When $\alpha = 0.01$, $N = M = 2$, $\beta \in (0.4, 1.1)$, and initial conditions are set as $[0.4, 0, 0, -0.4]$, the Lyapunov exponents and bifurcation diagram of system (1) are shown in Fig. 7.

It can be seen from Fig. 7(a) that, when $0.4 < \beta < 0.948$, $LE_1 > 0, LE_2 > 0, LE_3 \approx 0$ and $LE_4 < 0$. In other words, the system (1) has two positive Lyapunov exponents, a negative Lyapunov exponent and a Lyapunov exponent equal to 0, which indicates that the system (1) is hyperchaotic in this parameter space. When $\beta = 0.62$, the Lyapunov exponents are $LE_1 = 0.0837, LE_2 = 0.0791, LE_3 = 0$ and $LE_4 = -0.7728$, so the Lyapunov dimension is $D_L \approx 3.21$, which corresponds to a hyperchaotic attractor. As parameter β increases further, such as $0.948 \leq \beta < 0.993$, and then $LE_1 > 0, LE_2 \approx 0, LE_3 < 0, LE_4 < 0$, system (1) has only one positive Lyapunov exponent, so the system goes from hyperchaotic state to general chaotic state. Therefore, the dynamic behavior complexity of the system is reduced. It can also be seen from the Lyapunov dimension, that when $\beta = 0.96$, the Lyapunov exponents are $LE_1 = 0.0849, LE_2 = 0, LE_3 = -0.056$ and $LE_4 = -0.986$, so the Lyapunov dimension is $D_L \approx 3.03$, which corresponds to a general chaotic attractor.

As the system parameter further increases, when in interval $0.993 \leq \beta < 1.02$, the system has two Lyapunov exponents that are equal to 0 and two negative Lyapunov exponents, thus the corresponding Lyapunov dimension in this interval is $D_L = 2$, which corresponds to quasi-periodic attractor (torus). When $1.02 \leq \beta < 1.1$, the system has only one Lyapunov exponent that is equal to 0, others are negative and the corresponding Lyapunov dimension in this interval is $D_L = 1$, which corresponds to the periodic attractor (limit cycle). The above analysis results are further confirmed in Fig. 7(b). According to Figs. 7(a) and 7(b), when $0.4 < \beta < 0.948$, system (1) is a multiscroll hyperchaotic system, and when $0.948 < \beta < 0.993$, system (1) is a general multiscroll chaotic system. This is the innovation of the multiscroll hyperchaotic system designed in this paper, compared with the multiscroll chaotic system with hidden attractors proposed in [Chen & Yang, 2015], it has more complex dynamic characteristics.

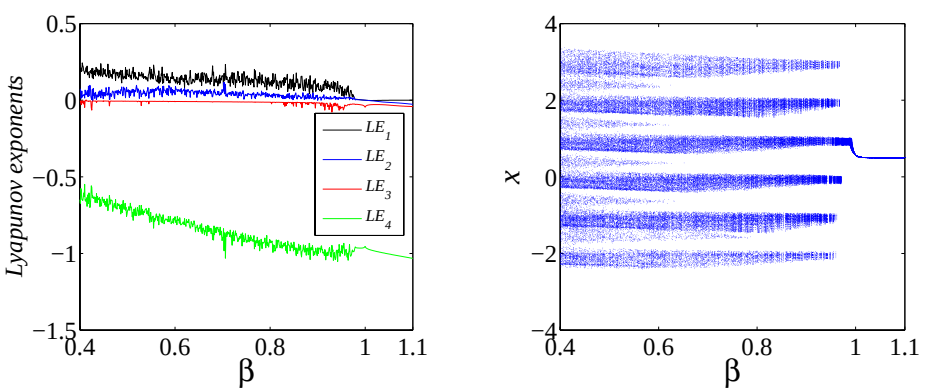

(a) (b)

Fig. 7. Lyapunov exponent and bifurcation diagram with the system parameters $\alpha = 0.01$, $N = M = 2$ and $0.4 < \beta < 1.1$, (a) Lyapunov exponent diagram and (b) bifurcation diagram, $\beta - x$.

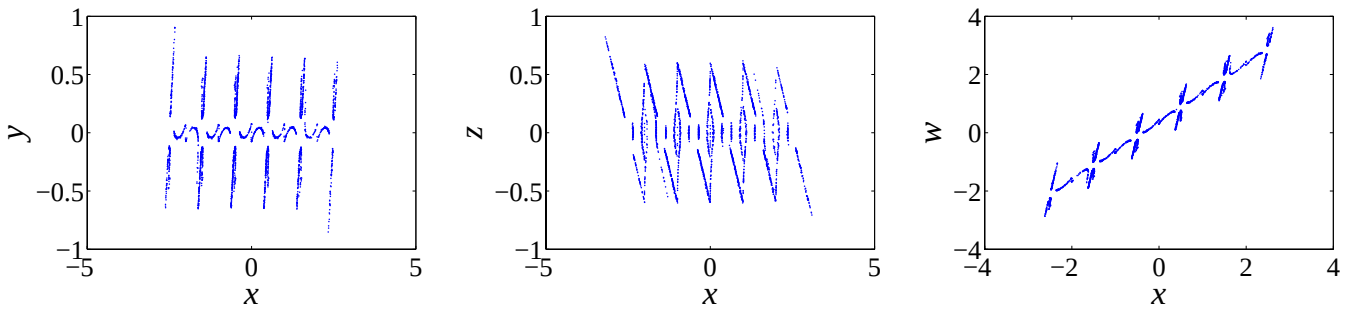

(a) (b) (c)

Fig. 8. Poincaré map in (a) x–y plane, $z = 0$, (b) x–z plane, $y = 0$ and (c) x–w plane, $z = 0$.

Figure 8 shows the Poincaré map diagram, in this diagram, the system parameters are $\alpha = 0.01$, $\beta = 0.62$ and $N = M = 2$. The Poincaré map of the system (1) in x–y, x–z and x–w planes are respectively shown in Figs. 8(a)–8(c). As can be seen from Figs. 8(a)–8(c), the Poincaré map of the system on different planes are a number of dense points and they are respectively very similar to Figs. 5(a)–5(c), which proves the characteristics of bifurcation and foldability that chaos possesses.

3.4. *Adaptive synchronization of the novel four-dimensional chaotic system*

The adaptive synchronization method enables the system to adjust its coupling strength along with the magnitude of error, which is more suitable for numerical simulation and actual system [Zhou *et al.*, 2008; Du *et al.*, 2018]. The estimation method of unknown parameters brought by adaptive synchronization method provides a good analysis tool for chaotic synchronization. In recent years, adaptive synchronization methods have been widely used in the study of chaotic synchronization [Vaidyanathan, 2016; Gao *et al.*, 2016]. Therefore, we give an adaptive synchronization example for the proposed multiscroll hyperchaotic system with hidden attractors.

The two multiscroll hyperchaotic systems with hidden attractors, we called them respectively master and slave systems, are described as follows. The master system is described as

$$\begin{cases} \dot{x}_1 = y_1, \\ \dot{y}_1 = z_1 - \alpha y_1 z_1 w_1, \\ \dot{z}_1 = -x_1 - y_1 - \beta z_1 + f(x_1, M, N), \\ \dot{w}_1 = y_1 + z_1, \end{cases} \tag{10}$$

while the slave system is

$$\begin{cases} \dot{x}_2 = y_2 + u_x, \\ \dot{y}_2 = z_2 - \alpha y_2 z_2 w_2 + u_y, \\ \dot{z}_2 = -x_2 - y_2 - \beta z_2 + f(x_2, M, N) + u_z, \\ \dot{w}_2 = y_2 + z_2 + u_w, \end{cases} \tag{11}$$

in which α and β are unknown system parameters. In Eq. (11), $u = [u_x, u_y, u_z, u_w]^T$ is the designed adaptive controller. The error function about all state variables of the master system and the slave system are expressed as $(e_x, e_y, e_z, e_w) = (x_1 - x_2, y_1 - y_2, z_1 - z_2, w_1 - w_2)$.

Because the system parameters α and β are unknown, for adaptive control method, we must estimate the error of the system parameters, they are represented as $(e_\alpha, e_\beta) = (\alpha - \alpha_1, \beta - \beta_1)$, where the estimations of the unknown parameters α and β are α_1 and β_1, respectively.

The designed adaptive controller is shown below

$$\begin{cases} u_x = e_y + \delta_x e_x, \\ u_y = e_z - \alpha_1(y_1 z_1 w_1 - y_2 z_2 w_2) + \delta_y e_y, \\ u_z = -e_x - e_y - \beta_1 e_z + \delta_z e_z, \\ u_w = e_y + e_z + \delta_w e_w, \end{cases} \tag{12}$$

where $\delta_x, \delta_y, \delta_z$ and δ_w are four positive gain constants. The system parameter update law in Eq. (12) is given by $(\dot{\alpha}_1, \dot{\beta}_1) = [-e_y(y_1 z_1 w_1 - y_2 z_2 w_2), -e_z^2]$.

Next, we verify the correctness of the designed adaptive controller. For this reason, we define a quadratic Lyapunov function

$$V(e_x, e_y, e_z, e_w, e_\alpha, e_\beta) = \frac{1}{2}(e_x^2 + e_y^2 + e_z^2 + e_w^2 + e_\alpha^2 + e_\beta^2). \tag{13}$$

The Lyapunov function is differentiated and the following equation is obtained

$$\dot{V} = e_x\dot{e}_x + e_y\dot{e}_y + e_z\dot{e}_z + e_w\dot{e}_w + e_\alpha\dot{e}_\alpha + e_\beta\dot{e}_\beta. \tag{14}$$

The error dynamics of the master system and the slave system can be expressed as

$$\begin{cases} \dot{e}_x = \dot{x}_1 - \dot{x}_2 = -\delta_x e_x, \\ \dot{e}_y = \dot{y}_1 - \dot{y}_2 = -e_\alpha(y_1 z_1 w_1 - y_2 z_2 w_2) - \delta_y e_y, \\ \dot{e}_z = \dot{z}_1 - \dot{z}_2 = -e_\beta e_z - \delta_z e_z, \\ \dot{e}_w = \dot{w}_1 - \dot{w}_2 = -\delta_w e_w. \end{cases} \tag{15}$$

We can get the corresponding dynamics of the parameter estimation errors $(\dot{e}_\alpha, \dot{e}_\beta) = (-\dot{\alpha}_1, -\dot{\beta}_1)$.

Based on the analyses above, one can get the differential form of the Lyapunov function

$$\dot{V} = -\delta_x e_x^2 - \delta_y e_y^2 - \delta_z e_z^2 - \delta_w e_w^2. \tag{16}$$

It is easy to see that the differential of the Lyapunov function is a negative semidefinite function. Therefore, it is simply to verify that $e_x \to 0, e_y \to 0, e_z \to 0$ and $e_w \to 0$ exponentially as $t \to \infty$ according to the Barbalat's lemma [Khalil, 2002]. Therefore, the synchronization between the master system and the slave system is obtained.

In order to verify the correctness of the designed adaptive controller and synchronization scheme, we take the 6-scroll hyperchaotic system with hidden attractors as an example to carry out the synchronization simulation experiment. The initial state of system state variables, the system parameters and the initial value of corresponding parameter estimation in the two systems are listed below

$$\begin{cases} x_1(0) = 0.4, \quad y_1(0) = 0, \\ z_1(0) = 0, \quad w_1(0) = 0.8, \\ x_2(0) = 0.2, \quad y_2(0) = 0.1, \\ z_2(0) = -0.1, \quad w_2(0) = 0.75, \\ \alpha = 0.01, \quad \beta = 0.62, \\ \alpha_1(0) = 0.03, \quad \beta_1(0) = 0.58. \end{cases} \tag{17}$$

The positive gain constants are selected as $\delta_x = \delta_y = \delta_z = \delta_w = 3$. Figure 9 shows the time-history of the synchronization errors e_x, e_y, e_z and e_w. From Fig. 9, we can see that the synchronization between the slave system and the master system is achieved.

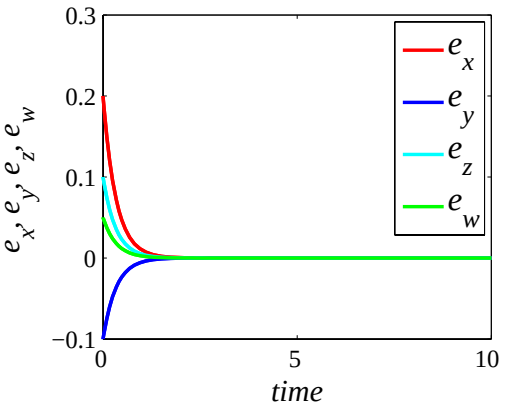

Fig. 9. Time-history of the synchronization errors between the master system and the slave system, when $x_1(0) = 0.4$, $y_1(0) = 0, z_1(0) = 0, w_1(0) = 0.8; x_2(0) = 0.2, y_2(0) = 0.1$, $z_2(0) = -0.1, w_2(0) = 0.75; \alpha = 0.01, \beta = 0.62; \alpha_1(0) = 0.03$, $\beta_1(0) = 0.58$.

4. Hardware Circuit Design and Experimental Results

In order to further verify the correctness of the proposed multiscroll hyperchaotic system with hidden attractors, the corresponding circuit experiments are carried out in this section. The designed hardware experimental circuit is shown in Fig. 10. The analog multiplier AD633JN and the operational amplifier TL082 are adopted in the circuit implementation. The power voltage of TL082 and AD633JN are set to ±15 V.

Let $v_{C1} = x, v_{C2} = y, v_{C3} = z$ and $v_{C4} = w$, of which v_{C1}, v_{C2}, v_{C3} and v_{C4} respectively represent the voltages across the capacitance C_1, C_2, C_3 and C_4 in Fig. 10. It is easy to get the state equation of the circuit shown in Fig. 10

$$\begin{cases} C_1 \cdot \dfrac{dx}{dt} = \dfrac{y}{R_1}, \\ C_2 \cdot \dfrac{dy}{dt} = \dfrac{z}{R_2} - 0.01 \cdot \dfrac{yzw}{R_3}, \\ C_3 \cdot \dfrac{dz}{dt} = -\dfrac{x}{R_4} - \dfrac{y}{R_5} - \dfrac{z}{R_6} + \dfrac{f(x)}{R_7}, \\ C_4 \cdot \dfrac{dw}{dt} = \dfrac{y}{R_8} + \dfrac{z}{R_9}. \end{cases} \tag{18}$$

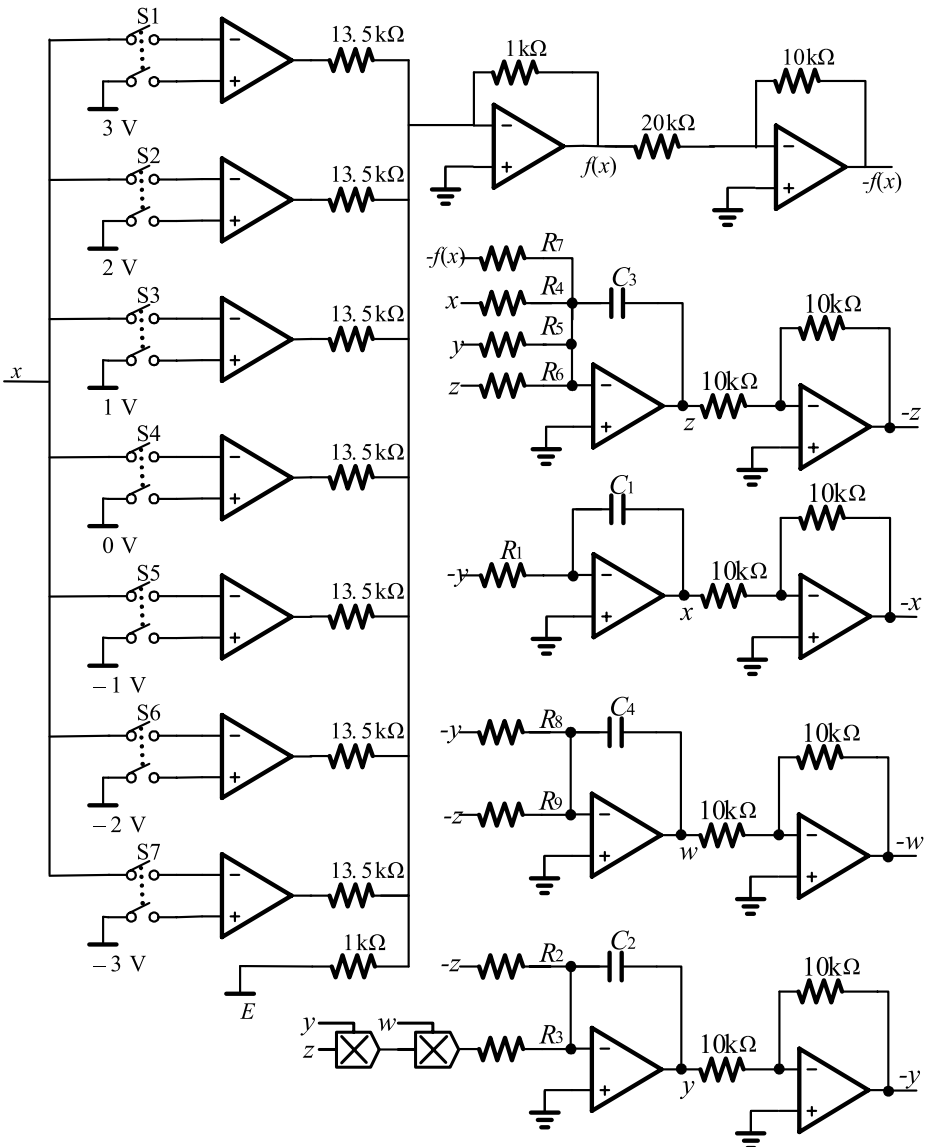

Fig. 10. Circuit diagram of multiscroll hyperchaotic system with hidden attractors.

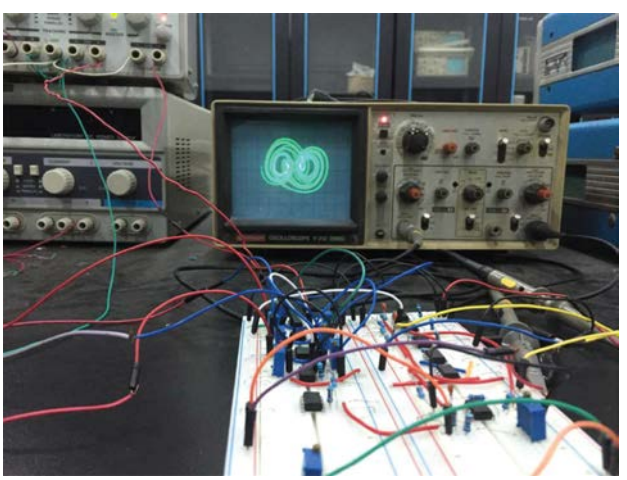

Fig. 11. Field picture of hardware circuit experiment.

The time factor $1/RC$ is introduced into Eq. (1)

$$\begin{cases} C \cdot \dfrac{dx}{dt} = \dfrac{y}{R}, \\ C \cdot \dfrac{dy}{dt} = \dfrac{z}{R} - \dfrac{\alpha yzw}{R}, \\ C \cdot \dfrac{dz}{dt} = -\dfrac{x}{R} - \dfrac{y}{R} - \dfrac{\beta z}{R} + \dfrac{f(x)}{R}, \\ C \cdot \dfrac{dw}{dt} = \dfrac{y}{R} + \dfrac{z}{R}. \end{cases} \tag{19}$$

Let $\alpha = 0.01$, $\beta = 0.62$, $C_1 = C_2 = C_3 = C_4 = 10\,\text{nF}$ and $R = 100\,\text{k}\Omega$, and compare Eqs. (18) and (19), one gets

$$\begin{cases} \dfrac{1}{R_1} = \dfrac{1}{R} \to R_1 = 100\,\text{k}\Omega, \\ \dfrac{1}{R_2} = \dfrac{1}{R} \to R_2 = 100\,\text{k}\Omega, \\ \dfrac{0.01}{R_3} = \dfrac{\alpha}{R} \to R_3 = 100\,\text{k}\Omega, \\ \dfrac{1}{R_4} = \dfrac{1}{R} \to R_4 = 100\,\text{k}\Omega, \\ \dfrac{1}{R_5} = \dfrac{1}{R} \to R_5 = 100\,\text{k}\Omega, \\ \dfrac{1}{R_6} = \dfrac{\beta}{R} \to R_6 = 161.3\,\text{k}\Omega, \\ \dfrac{1}{R_7} = \dfrac{1}{R} \to R_7 = 100\,\text{k}\Omega, \\ \dfrac{1}{R_8} = \dfrac{1}{R} \to R_8 = 100\,\text{k}\Omega, \\ \dfrac{1}{R_9} = \dfrac{1}{R} \to R_9 = 100\,\text{k}\Omega. \end{cases} \tag{20}$$

The photo of the experimental site is shown in Fig. 11. The relationship between the number of scrolls and the on-off set of switch is listed in Table 1, which contains ten kinds of circumstances. For the circuit in *Case* 1, *Case* 2, *Case* 4, and setting the corresponding value of the comparison voltage E, the 2-scroll, 3-scroll and 4-scroll hidden attractors chaotic phase portraits can be observed. The experimental circuit results of hidden attractor chaotic phase portraits in x–y and x–z plane are shown in Fig. 12.

Comparing Figs. 12(a) and 12(b) and Figs. 1(a) and 1(b), Figs. 12(c) and 12(d) and Figs. 2(a) and 2(b), Figs. 12(e) and 12(f) and Figs. 3(a) and 3(b), we can see that the MATLAB simulation results and the circuit experimental results are consistent. This proves the correctness of the proposed multi-scroll hyperchaotic system with hidden attractors.

5. Relevant Literature Comparison

The relevant literature comparison is shown in Table 2. The number of scrolls generated by the hyperchaotic systems with hidden attractors that were published in [Wang *et al.*, 2012; Khan & Shikha, 2018; Singh & Roy, 2018; Zhou & Yang, 2013; Chen & Yang, 2015] are limited, at most, only 2-scroll hidden attractors can be generated, and no hardware circuit verifications have been carried out. The multiscroll chaotic system with hidden attractors proposed in literature [Hu *et al.*, 2016] can generate any number of scroll hidden attractors only in numerical simulation. However, when the circuit is implemented, it is limited to sine function electronic devices and only a limited number of scrolls can be generated. Therefore, this chaotic system is a kind of multiscroll chaotic system with limited number of scrolls; in addition, this multiscroll chaotic system

Table 1. Relationship between the number of scrolls with the on-off set of switch.

	S_1	S_2	S_3	S_4	S_5	S_6	S_7	E/V	Number of Scrolls
Case 1	off	off	off	**on**	off	off	off	0	2
Case 2	off	off	**on**	**on**	off	off	off	1	3
Case 3	off	off	off	**on**	**on**	off	off	−1	3
Case 4	off	off	**on**	**on**	**on**	off	off	0	4
Case 5	off	**on**	**on**	**on**	**on**	off	off	1	5
Case 6	off	off	**on**	**on**	**on**	**on**	off	−1	5
Case 7	off	**on**	**on**	**on**	**on**	**on**	off	0	6
Case 8	**on**	**on**	**on**	**on**	**on**	**on**	off	1	7
Case 9	off	**on**	**on**	**on**	**on**	**on**	**on**	−1	7
Case 10	**on**	**on**	**on**	**on**	**on**	**on**	**on**	0	8

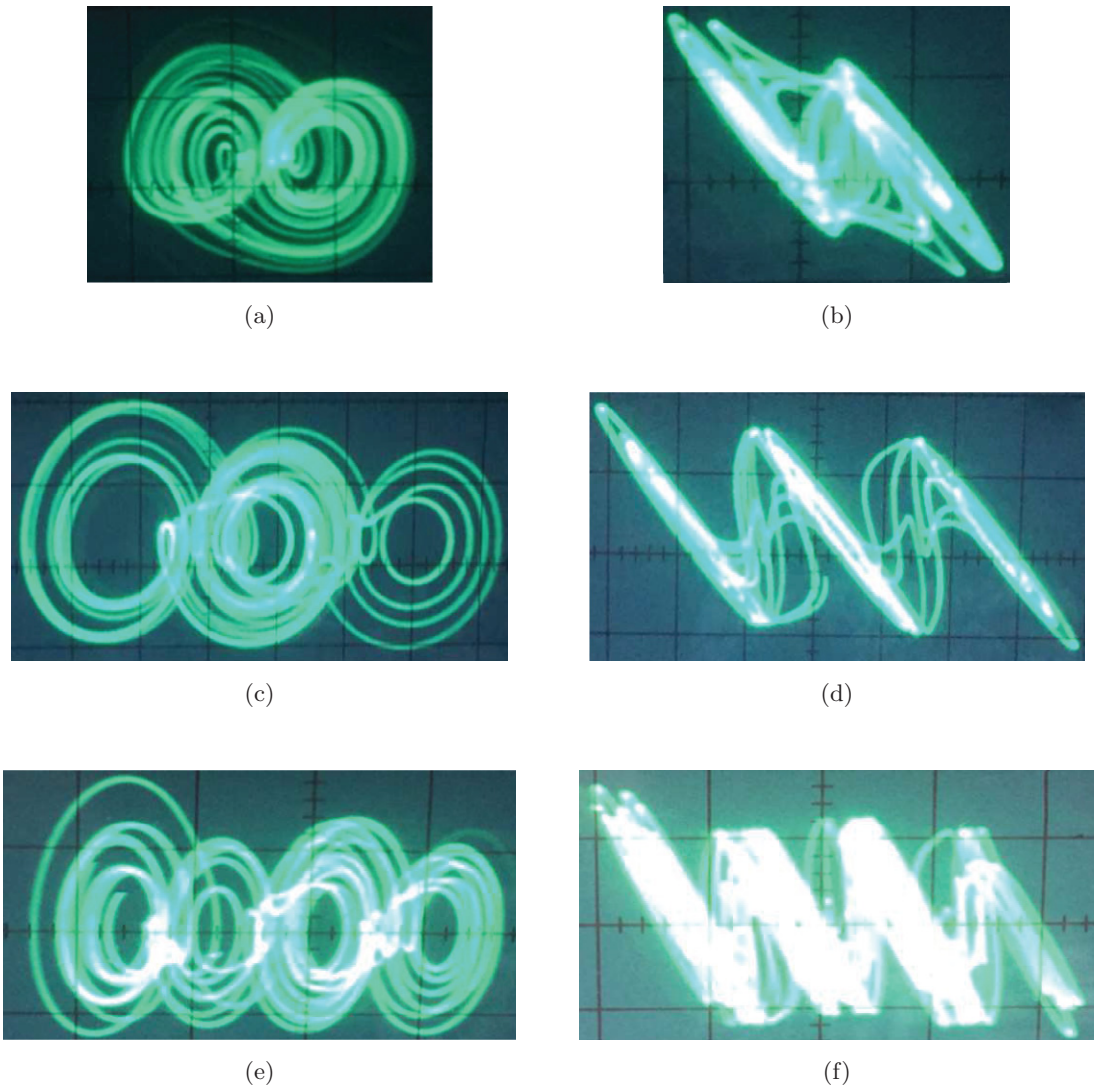

Fig. 12. Hardware experimental results of multiscroll hyperchaotic circuit with hidden attractors. In which, phase portraits of 2-scroll hyperchaotic hidden attractors are shown in (a) x–y and (b) x–z plane; phase portraits of 3-scroll hyperchaotic hidden attractors are shown in (c) x–y and (d) x–z plane; phase portraits of 4-scroll hyperchaotic hidden attractors are shown in (e) x–y and (f) x–z plane (where $x = y = z = 0.5\,\mathrm{V/div}$).

Table 2. Related literature comparison.

Literature	Number of Scrolls	Complexity of the System	Hardware Experiment	Published Year
[Wang *et al.*, 2012]	Single Scroll	Hyperchaotic	No	2012
[Zhou & Yang, 2013]	2-Scroll	Hyperchaotic	No	2013
[Chen & Yang, 2015]	2-Scroll	Hyperchaotic	No	2015
[Khan & Shikha, 2018]	2-Scroll	Hyperchaotic	No	2018
[Singh & Roy, 2018]	2-Scroll	Hyperchaotic	No	2018
[Hu *et al.*, 2016]	Limited	Chaotic	No	2016
[Hu *et al.*, 2017]	Limited	Chaotic	No	2017
[Escalante-Gonzalez *et al.*, 2017]	Arbitrary	Chaotic	No	2017
This paper	**Arbitrary**	**Hyperchaotic**	**Yes**	—

with hidden attractors is not a hyperchaotic system. In literature [Hu *et al.*, 2017], a multiscroll chaotic system with hidden attractor is designed based on memristor and sine function, and the same problem is encountered as in literature [Hu *et al.*, 2016], the proposed system is a multiscroll chaotic system with limited number of scrolls and it is not a hyperchaotic system. The multiscroll chaotic system with hidden attractors designed in literature [Escalante-Gonzalez *et al.*, 2017] can generate any number of scroll hidden attractors, but it is not a hyperchaotic system and no hardware experiment has been carried out.

By comparison, the chaotic system proposed in this paper can generate hidden attractors with any number of scrolls and it is a hyperchaotic system with more complex dynamic characteristics, therefore, it is more suitable for chaotic secure communications, image encryption, and so on. In addition, the hardware experiments are also carried out using discrete components.

6. Conclusion

Based on Jerk chaotic system, a multiscroll hyperchaotic system with hidden attractors that can generate any number of scrolls is proposed. The numerical simulations of the system are given by MATLAB simulation, including the phase portraits of 2-, 3-, 4-, 5-, 6- and 13-scroll hyperchaotic hidden attractors. The dynamic characteristics of the multiscroll hyperchaotic system with hidden attractors are analyzed by means of dynamic analysis methods such as Lyapunov exponent and bifurcation diagram. An adaptive synchronous numerical simulation is carried out for the proposed chaotic system. The hardware experiment of the proposed multiscroll hyperchaotic system with hidden attractors is carried out using discrete components, the hyperchaotic phase portraits of 2-, 3- and 4-scroll hidden attractors are generated, and the experimental results are consistent with the MATLAB simulation results. Finally, by comparing the relevant literatures, we find that the reported hyperchaotic systems with hidden attractors can only generate 2-scroll hidden attractors, but the hyperchaotic system with hidden attractors proposed in this paper can generate $N + M + 2$ scroll hyperchaotic hidden attractors; other reported multiscroll chaotic systems with hidden attractors are not hyperchaotic systems, while the proposed multiscroll chaotic system with hidden attractors is a hyperchaotic system, and the whole circuit has a simple structure. It is worth noting that the simple step sequence is adopted in our work to generate multiscroll attractors. However, in order to generate more chaotic attractors with different shapes in the proposed chaotic system, the nonlinear functions in the proposed chaotic system can be replaced by piecewise-linear sequence [Yu *et al.*, 2007], saturation sequence [Zhang & Wang, 2018], and hysteresis sequence [Zhang & Yu, 2009; Lü *et al.*, 2006]. And the corresponding equilibrium calculation and simulation test are carried out and proved to be feasible.

Acknowledgments

The authors would like to thank the editors and anonymous reviewers for their valuable comments which have helped in improving this paper. This research was supported by the National Natural Science Foundation of China (No. 61571185), the Science and Technology Planning Project of Hunan Province (No. 2017GK4009), and the Open Fund Project of Key Laboratory in Hunan Universities (No. 18K010).

References

Bao, B. C., Jiang, T., Wang, G. Y., Jin, P. P., Bao, H. & Chen, M. [2017] "Two-memristor-based Chua's hyperchaotic circuit with plane equilibrium and its extreme multistability," *Nonlin. Dyn.* **89**, 1157–1171.

Bao, B. C., Hu, A. H., Bao, H., Xu, Q., Chen, M. & Wu, H. G. [2018] "Three-dimensional memristive Hindmarsh–Rose neuron model with hidden coexisting asymmetric behaviors," *Complexity* **4**, 3872573.

Borah, M. & Roy, B. K. [2017] "Hidden attractor dynamics of a novel non-equilibrium fractional-order chaotic system and its synchronisation control," *3rd Indian Control Conf.*, pp. 450–455.

Boriga, R., Dăscălescu, A. C. & Priescu, I. [2014] "A new hyperchaotic map and its application in an image encryption scheme," *Sign. Process.-Image Commun.* **29**, 887–901.

Chen, Y. M. & Yang, Q. G. [2015] "A new Lorenz-type hyperchaotic system with a curve of equilibria," *Math. Comput. Simul.* **112**, 40–55.

Chua, L. O., Komuro, M. & Matsumoto, T. [1986] "The double scroll family," *IEEE Trans. Circuits Syst.* **33**, 1072–1118.

Du, L., Yang, Y. & Lei, Y. M. [2018] "Synchronization in a fractional-order dynamic network with uncertain parameters using an adaptive control strategy," *Appl. Math. Mech.-Engl. Ed.* **39**, 353–364.

Escalante-Gonzalez, R. J., Campos-Canton, E. & Nicol, M. [2017] "Generation of multiscroll attractors without equilibria via piecewise linear systems," *Chaos* **27**, 053109.

Filali, R. L., Benrejeb, M. & Borne, P. [2014] "On observer-based secure communication design using discrete-time hyperchaotic systems," *Commun. Nonlin. Sci. Numer. Simul.* **19**, 1424–1432.

Gao, X. J., Cheng, M. F. & Hu, H. P. [2016] "Adaptive impulsive synchronization of uncertain delayed chaotic system with full unknown parameters via discrete-time drive signals," *Complexity* **21**, 43–51.

Gotthans, T. & Petrzela, J. [2015] "New class of chaotic systems with circular equilibrium," *Nonlin. Dyn.* **81**, 1–7.

Gotthans, T., Sprott, J. C. & Petrzela, J. [2016] "Simple chaotic flow with circle and square equilibrium," *Int. J. Bifurcation and Chaos* **26**, 1650137-1–8.

Hu, X. Y., Liu, C. X., Liu, L., Ni, J. K. & Li, S. L. [2016] "Multi-scroll hidden attractors in improved Sprott A system," *Nonlin. Dyn.* **86**, 1725–1734.

Hu, X. Y., Liu, C. X., Liu, L., Yao, Y. P. & Zheng, G. C. [2017] "Multi-scroll hidden attractors and multi-wing hidden attractors in a 5-dimensional memristive system," *Chin. Phys. B* **26**, 120–126.

Jafari, S. & Sprott, J. C. [2013] "Simple chaotic flows with a line equilibrium," *Chaos Solit. Fract.* **57**, 79–84.

Jafari, S., Sprott, J. C. & Golpayegani, S. M. R. H. [2013] "Elementary quadratic chaotic flows with no equilibria," *Phys. Lett. A* **377**, 699–702.

Khalil, H. K. [2002] *Nonlinear Systems*, 3rd edition (Prentice-Hall, Upper Saddle River, NJ, USA).

Khan, A. & Shikha [2018] "Chaotic analysis and combination-combination synchronization of a novel hyperchaotic system without any equilibria," *Chin. J. Phys.* **56**, 238–251.

Leonov, G. A., Kuznetsov, N. V. & Vagaitsev, V. I. [2011] "Localization of hidden Chua's attractors," *Phys. Lett. A* **375**, 2230–2233.

Leonov, G. A., Kuznetsov, N. V. & Vagaitsev, V. I. [2012] "Hidden attractor in smooth Chua system," *Physica D* **241**, 1482–1486.

Leonov, G. A. & Kuznetsov, N. V. [2013] "Hidden attractors in dynamical systems. From hidden oscillations in Hilbert–Kolmogorov, Aizerman, and Kalman problems to hidden chaotic attractor in Chua circuits," *Int. J. Bifurcation and Chaos* **23**, 1–69.

Leonov, G. A., Kuznetsov, N. V., Kiseleva, M. A., Solovyeva, E. P. & Zaretskiy, A. M. [2014] "Hidden oscillations in mathematical model of drilling system actuated by induction motor with a wound rotor," *Nonlin. Dyn.* **77**, 277–288.

Lorenz, E. N. [1963] "Deterministic non-periodic flow," *J. Atmos. Sci.* **20**, 130–141.

Lü, J. H., Yu, S. M., Leung, H. & Chen, G. R. [2006] "Experimental verification of multidirectional multiscroll chaotic attractors," *IEEE Trans. Circuits Syst.-I: Regul. Pap.* **53**, 149–165.

Molaie, M., Jafari, S., Sprott, J. C. & Golpayegani, S. [2013] "Simple chaotic flows with one stable equilibrium," *Int. J. Bifurcation and Chaos* **23**, 1350188-1–7.

Pham, V. T., Vaidyanathan, S., Volos, C. & Jafari, S. [2015] "Hidden attractors in a chaotic system with an exponential nonlinear term," *Eur. Phys. J. Special Topics* **224**, 1507–1517.

Pham, V. T., Jafari, S., Wang, X. & Ma, J. [2016a] "A chaotic system with different shapes of equilibria," *Int. J. Bifurcation and Chaos* **26**, 1650069-1–5.

Pham, V. T., Jafari, S., Volos, C. & Kapitaniak, T. [2016b] "A gallery of chaotic systems with an infinite number of equilibrium points," *Chaos Solit. Fract.* **93**, 58–63.

Pham, V. T., Jafari, S., Volos, C. & Kapitaniak, T. [2017a] "Different families of hidden attractors in a new chaotic system with variable equilibrium," *Int. J. Bifurcation and Chaos* **27**, 1750138-1–10.

Pham, V. T., Wang, X., Jafari, S., Volos, C. & Kapitaniak, T. [2017b] "From Wang–Chen system with only one stable equilibrium to a new chaotic system without equilibrium," *Int. J. Bifurcation and Chaos* **27**, 1750097-1–9.

Singh, J. P. & Roy, B. K. [2018] "Hidden attractors in a new complex generalised Lorenz hyperchaotic system, its synchronisation using adaptive contraction theory, circuit validation and application," *Nonlin. Dyn.* **92**, 373–394.

Sprott, J. C. [2000] "Simple chaotic systems and circuits," *Am. J. Phys.* **68**, 758–763.

Swathy, P. S. & Thamilmaran, K. [2014] "Hyperchaos in SC-CNN based modified canonical Chua's circuit," *Nonlin. Dyn.* **78**, 2639–2650.

Vaidyanathan, S. [2016] "Hyperchaos, adaptive control and synchronization of a novel 4-D hyperchaotic system with two quadratic nonlinearities," *Arch. Contr. Sci.* **26**, 471–495.

Wang, X. & Chen, G. [2012] "A chaotic system with only one stable equilibrium," *Commun. Nonlin. Sci. Numer. Simul.* **17**, 1264–1272.

Wang, Z. H., Cang, S. J., Ochola, E. O. & Sun, Y. X. [2012] "A hyperchaotic system without equilibrium," *Nonlin. Dyn.* **69**, 531–537.

Wang, X. Y. & Zhang, H. L. [2016] "A novel image encryption algorithm based on genetic recombination and hyper-chaotic systems," *Nonlin. Dyn.* **83**, 333–346.

Wang, C. H., Liu, X. M. & Xia, H. [2017a] "Multi-piecewise quadratic nonlinearity memristor and its 2N-scroll and 2N+1-scroll chaotic attractors system," *Chaos* **27**, 033114.

Wang, X., Pham, V. T., Jafari, S., Volos, C., Munoz-Pacheco, J. M. & Tlelo-Cuautle, E. [2017b] "A new chaotic system with stable equilibrium: From theoretical model to circuit implementation," *IEEE Access* **5**, 8851–8858.

Wang, Y., Wang, C. H. & Zhou, L. [2017c] "A time-delayed hyperchaotic system composed of multiscroll attractors with multiple positive Lyapunov exponents," *J. Comput. Nonlin. Dyn.* **12**, 051029.

Wolf, A., Swift, J. B., Swinney, H. L. & Vastano, J. A. [1985] "Determining Lyapunov exponents from a time series," *Physica D* **16**, 285–317.

Wu, X. J., Fu, Z. Y. & Kurths, J. [2015] "A secure communication scheme based generalized function projective synchronization of a new 5D hyperchaotic system," *Phys. Scr.* **90**, 045210.

Yu, S. M., Lü, J. H. & Chen, G. R. [2007] "A family of n-scroll hyperchaotic attractors and their realization," *Phys. Lett. A* **364**, 244–251.

Zhang, C. X. & Yu, S. M. [2009] "Design and implementation of a novel multiscroll chaotic system," *Chin. Phys. B* **18**, 119–129.

Zhang, C. X. & Yu, S. M. [2013] "On constructing complex grid multiwing hyperchaotic system: Theoretical design and circuit implementation," *Int. J. Circuit Th. Appl.* **38**, 221–237.

Zhang, G. T. & Wang, F. Q. [2018] "A novel multiscroll chaotic generator: Analysis, simulation, and implementation," *Chin. Phys. B* **27**, 018201.

Zhang, S., Zeng, Y. C., Li, Z. J., Wang, M. J. & Xiong, L. [2018] "Generating one to four-wing hidden attractors in a novel 4D no-equilibrium chaotic system with extreme multistability," *Chaos* **28**, 013113.

Zhang, X. & Wang, C. H. [2019] "A novel multi-attractor period multiscroll chaotic integrated circuit based on CMOS wide adjustable CCCII," *IEEE Access* **7**, 16336–16350.

Zhou, J., Lu, J. A. & Lü, J. H. [2008] "Pinning adaptive synchronization of a general complex dynamical network," *Automatica* **44**, 996–1003.

Zhou, P. & Yang, F. Y. [2013] "Hyperchaos, chaos, and horseshoe in a 4D nonlinear system with an infinite number of equilibrium points," *Nonlin. Dyn.* **76**, 473–480.

Zhou, P., Huang, K. & Yang, C. D. [2013] "A fractional-order chaotic system with an infinite number of equilibrium points," *Discr. Dyn. Nat. Soc.* **3**, 331–372.

Zhou, L., Wang, C. H. & Zhou, L. L. [2016] "Generating hyperchaotic multiwing attractor in a 4D memristive circuit," *Nonlin. Dyn.* **85**, 2653–2663.

Zhou, L., Wang, C. H. & Zhou, L. L. [2017] "Generating four-wing hyperchaotic attractor and two-wing, three-wing, and four-wing chaotic attractors in 4D memristive system," *Int. J. Bifurcation and Chaos* **27**, 1750027-1–14.

Zhou, L., Wang, C. H., Zhang, X. & Yao, W. [2018a] "Various attractors, coexisting attractors and antimonotonicity in a simple fourth-order memristive twin-T oscillator," *Int. J. Bifurcation and Chaos* **28**, 1850050-1–18.

Zhou, L., Wang, C. H. & Zhou, L. L. [2018b] "A novel no-equilibrium hyperchaotic multiwing system via introducing memristor," *Int. J. Circuit Th. Appl.* **46**, 84–98.